

# Carmine Adsorption from Aqueous Solution by Crosslinked Peanut Husk

**Song, Yinghua\*<sup>+</sup>**

*Department of Chemistry and Chemical Engineering, Chongqing Technology and Business University,  
Chongqing 400067, CHINA*

**Liu, Yi**

*Voith Corporate Management Co., Ltd, Shanghai, 200120, CHINA*

**Chen, Shengming; Qin, Hongxia; Xu, Hui**

*Department of Chemistry and Chemical Engineering, Chongqing Technology and Business University,  
Chongqing 400067, CHINA*

**ABSTRACT:** *To observe the feasibility of the removal of carmine, peanut husk, an agriculture by-product, was crosslinked with epichlorohydrin in alkaline medium and used for adsorption of carmine from aqueous solution. Batch experiments were carried out to study the effects of various parameters such as initial pH, contact time, adsorbent dosage and initial carmine concentration as well as temperature on carmine adsorption. The results indicated that adsorption equilibrium data could be more effectively described by Langmuir isotherm equation than by Freundlich equation. The maximum monolayer adsorption capacity of peanut husk from the Langmuir model was 6.68 mg/g at 323 K. The pseudo second-order model provided a better fit to experimental data in the kinetic studies. The mass transfer model such as the intraparticle diffusion was applied to the experimental data to examine the mechanisms of the rate-controlling step. It was found that the intraparticle diffusion is the significant controlling step under the experimental conditions but it was not the unique one. The thermodynamic parameters of the adsorption process were also calculated by using constants derived from Langmuir equations, which propose an endothermic physical spontaneous adsorption process.*

**KEY WORDS:** *Peanut husk, Adsorption, Carmine, Isotherm, Kinetics, Thermodynamics.*

## INTRODUCTION

The dye based industrial wastewaters which were discharged from many industries, such as textiles, paper, leather, plastics, printing and cosmetics, have to be treated due to their impacts on water bodies. More and

more people realize the toxicity and carcinogenicity of dye-based based industrial wastewaters[1-3]. But many dyes are difficult to be degraded because of their complex aromatic species and xenobiotic properties. The removal

---

\* To whom correspondence should be addressed.

+ E-mail: yhswwjyhs@126.com

1021-9986/14/4/69

9\$/2.90

of synthetic dyes has become an important portion of dyes-based wastewater treatment. There are several methods to remove dyes such as treating dyes-containing wastewaters with physical and chemical processes. Nowadays activated carbon works as adsorbent to remove dyes in the wastewater in most commercial systems because of its high adsorption ability. But the processing costs are expensive. So people try to develop cheaper and effective adsorbents to remove dyes and find an alternative method from different starting materials such as bagasse pith[2], clay [4], saw dust [5], mango seed kernel[6], wheat straw[7], apple pomace [7], peanut husk [8-10], etc.

Peanut husk, an agricultural-by-products available in large quantity in china, often burned and discarded directly, which produce waste gas and dust. Fortunately, a possible solution has been found to utilize peanut husk as an adsorbent to remove contaminants from waste water. Peanut husk was introduced directly as a low-cost adsorbent for the efficient removal of Sunset Yellow dye from aqueous solution [11]. However, raw peanut husk cannot be used as a good natural adsorbent due to two major limitations. First, on contact with water, there is a leaching of yellowish color into solutions. Second, on prolonged contact with water, peanut husk tends to disintegrate. Researchers have studied the removal of heavy metals [12], phenol [13] and dyes [14] by partially carbonized peanut husk or by activated carbon from peanut husk. The purpose of this work was to produce a new adsorbent from peanut husk chemically crosslinked with epichlorohydrin in alkaline medium and the adsorption of carmine on it was investigated. The experiments were done in the same batch system to evaluate the adsorption capacity of the adsorbent, and the adsorption of carmine was studied on account of the initial carmine concentration, pH, adsorbent dosage, particle size and temperature. The equilibrium of adsorption was modeled with the Langmuir and Freundlich isotherms. The kinetic parameters and intraparticle diffusion were also determined for this process. Finally thermodynamic parameters such as Gibbs free energy change, isosteric enthalpy change and entropy change have also been calculated.

## EXPERIMENTAL SECTION

### *Preparation of Chemically Crosslinked Peanut Husk (CPH)*

The peanut husk used in this study was obtained from a farmers' market in Chongqing, Rep. of China.

The peanut husk was sieved into 40-60 meshes before modification. 2.0 g of the raw peanut husk was mixed with a solution of NaOH (45 mL, 1 mol/L) and epichlorohydrin (30 mL), then the mixture reacted for 1.5 h at  $(55 \pm 1)$  °C. The Crosslinked Peanut Husk (CPH) was rinsed with distilled water to remove residual materials and then oven-dried and stored in a desiccator.

### *Chemicals*

Stock solution was prepared by dissolving 0.1 g carmine in 1000 mL of twice-distilled water. The test solutions were prepared by diluting to the desired concentrations. All reagents used in this study were analytical reagent grade. The initial pH was adjusted to the pre-determined value using NaOH or HCl solutions prior to addition of adsorbent.

### *Batch adsorption studies*

Batch adsorption experiments were conducted in 150mL conical flasks containing different amount of CPH (0.2 - 1.0 g) and 100 mL of carmine solutions at the desired concentration, different pH values (2 - 12) and the constant temperature. The flasks were agitated on a shaker at 150 rpm constant shaking rate. Samples were taken from mixture during stirring at pre-determined time intervals to determine the residual color concentration in the system. The samples were centrifuged and the supernatant liquid was analyzed for the remaining color. All the experiments were carried out twice in parallel and average values were calculated further. For isotherms studies, a series of flasks containing 100mL carmine solution in the range of 10 - 50 mg/L were prepared. The weighed amount of 0.2 g CPH was added to each flask and then the mixtures were agitated at temperature of 30, 40 and 50°C respectively. These experiments were carried out at a constant pH of  $2.0 \pm 0.1$  for duration of 24 h.

The adsorption capacity  $q$  (mg/g) and the percent removal efficiency %R were calculated respectively as follows:

$$q = \frac{v(c_0 - c_t)}{m} \quad (1)$$

$$\%R = \frac{(c_0 - c_t)}{c_0} \times 100 \quad (2)$$

where  $c_0$  and  $c_e$  are the initial and the equilibrium concentrations (mg/L);  $v$  is the volume of carmine

solution used (L); and  $m$  is the mass of the dry CPH used(g).

### Analysis

The concentration of residual color of carmine in the adsorption system was determined spectrophotometrically. The absorbance of the color was measured at 508 nm.

### Adsorption isotherms and thermodynamic parameters

There are several variation types of adsorption isotherms. Langmuir and Freundlich isotherms which are most widely used since they can be applied to a wide range of adsorbate concentrations. The linear form of the Langmuir equation is generally accepted in the following variation:

$$\frac{c_e}{q_e} = \frac{1}{K_L q_{\max}} + \frac{c_e}{q_{\max}} \quad (3)$$

where  $c_e$  is the equilibrium concentration of dye solution(mg/L),  $q_e$  is the equilibrium capacity of dye on the adsorbent (mg/g),  $q_{\max}$  is the maximum monolayer adsorption capacity of the adsorbent (mg/g), and  $K_L$  is the Langmuir adsorption constant (L/mg).

The Freundlich isotherm equation is a semi-empirical one employed to describe heterogeneous system:

$$\ln q_e = \ln k_F + \frac{1}{n} \ln C_e \quad (4)$$

where  $k_F$  (L·mg<sup>-1</sup>) and  $n$  (dimensionless) are the Freundlich adsorption isotherm constants, indicating the capacity and intensity of the adsorption, respectively.

Thermodynamic parameters indicate energy transformation in the adsorption process, which can estimate the effect of temperature on carmine removal. Thermodynamic parameters, namely, Gibbs free energy values  $\Delta G$  (J/mol), the isosteric enthalpy change  $\Delta H$  (J/mol) and entropy change  $\Delta S$  (J/mol·K) at different temperature were calculated by the following equations[15,16]:

$$\Delta G = -RT \ln K \quad (5)$$

$$\ln(1/c_e) = \left(\frac{-\Delta H}{RT}\right) + \text{const} \tan t \quad (6)$$

$$\Delta S = \frac{\Delta H - \Delta G}{T} \quad (7)$$

where  $R$  is the universal gaseous constant(8.314 J/mol·K),  $T$  is the absolute temperature(K), and  $K$  is the equilibrium constant.

It is well known the unit for  $\Delta G$  is J/mol. Since the unit for the term  $RT$  is also J/mol, the  $K$  in Eq.(6) must be dimensionless. The present study was investigated in aqueous solution and  $K_L$  (the Langmuir constant) is given in L/mg, the  $K$  can be easily recalculated to become dimensionless by multiplying it by  $10^6$ (number of mgs of water per liter of solution, since the solution density is approximately 1 g/mL). Accordingly, the  $\Delta G$  value should be obtained from:

$$\Delta G = -RT \ln(10^6 K_L) \quad (8)$$

The term  $10^6 K_L$  (L/mg) (mg/L) is dimensionless.

### Adsorption Kinetics

In order to examine the controlling mechanism of adsorption processes such as mass transfer and chemical reaction, pseudo-first order, pseudo-second order and intraparticle diffusion kinetic equations were used to correlate the experimental data. The pseudo- first order kinetic model was suggested by Lagergren [17] for the adsorption of solid/liquid systems and its integrated form is given below:

$$\ln(q_e - q_t) = \ln q_e - k_1 t \quad (9)$$

where  $q_t$ (mg/g) is the adsorption capacity at time  $t$ (min<sup>-1</sup>) and  $k_1$  (min) is the rate constant of the pseudo-first adsorption.

The kinetic data were further analyzed with Ho's pseudo-second order kinetics model [18]. This model is based on the assumption that the adsorption follows second-order chemiadsorption. Its integrated linear form can be expressed as:

$$\frac{t}{q_t} = \frac{t}{q_e} + \frac{1}{k_2 q_e^2} \quad (10)$$

The adsorption of carmine onto CPH follows generally three consecutive steps of external diffusion, intraparticle diffusion and actual adsorption. One or more of these steps control the adsorption kinetics altogether or individually. In a completely agitated batch system, the external diffusion resistance is minimal, and the intraparticle diffusion is more likely to be the rate controlling step [19]. The kinetic data can also be analyzed by intraparticle diffusion kinetics model [20], as described below:

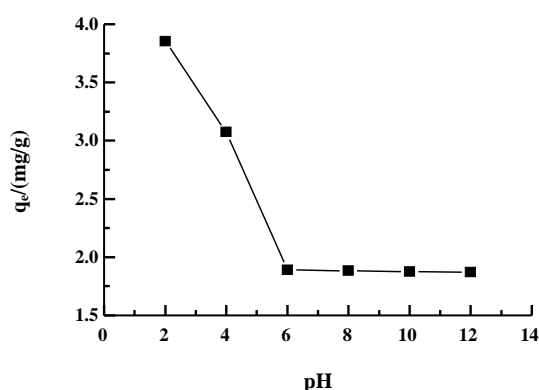


Fig. 1: Effect of pH ( $T = 30\text{ }^{\circ}\text{C}$ ,  $c_0 = 30\text{ mg/L}$ , CPH dosage = 5 g/L, rpm = 150).

$$q_t = k_p t^{1/2} + C \quad (11)$$

where  $k_p$  ( $\text{mg}/\text{min}^{1/2}\cdot\text{g}$ ) is the intraparticle diffusion rate constant and  $C$  ( $\text{mg}/\text{g}$ ) is a constant. where  $k_2$  ( $\text{g}/\text{mg}\cdot\text{min}$ ) is the rate constant of the pseudo-second-order adsorption.

For elucidation of the adsorption rate controlling mechanism, a mathematical model was also proposed to give the intraparticle diffusion coefficient. Intraparticle diffusion coefficient,  $D$  ( $\text{cm}^2/\text{s}$ ), may simply be calculated from the Wünlwald-Wagner intraparticle diffusion model [21]:

$$\lg\left(1 - \frac{q_t}{q_e}\right) = \lg\left(\frac{6}{\pi^2}\right) - \frac{4\pi^2 D}{2.303d^2} t \quad (12)$$

## RESULTS AND DISCUSSION

### Effect of Initial pH of solution

The pH value of the solution is an important factor that must be considered in the adsorption process. The initial pH of the working solutions has been adjusted between pH 2-12 by addition of diluting HCl and NaOH solution. The effect of pH on the adsorption of carmine was shown in Fig. 1.

As shown in Fig.1, a sharp decrease in the adsorption capacity occurs as the pH of the initial solution was increased from 2.0 up to 6.0 beyond which the rate of adsorption remains almost constant. For the subsequent studies, pH 2.0 was selected as an optimal pH value.

The higher adsorption of carmine at lower pH may be due to the enhanced protonation by neutralization of negative charge at the surface of the CPH. It contributed

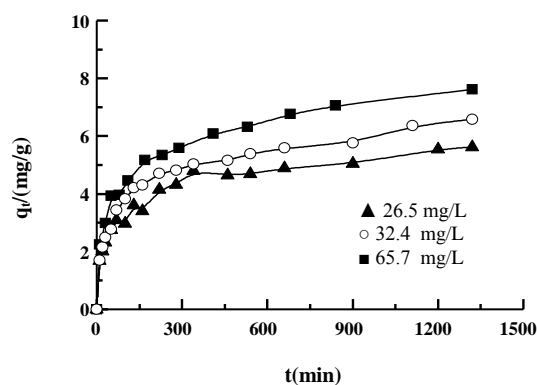


Fig. 2: Effect of initial carmine concentration ( $T = 30\text{ }^{\circ}\text{C}$ , pH = 2.0, CPH dosage = 2g/L, rpm = 150).

to the preferential adsorption of the dye over active sites and facilitates the diffusion process in the working solution. With increasing pH, protonation reduces and electrostatic repulsive force becomes dominant, which inhibits diffusion and adsorption.

### Effect of initial carmine concentration

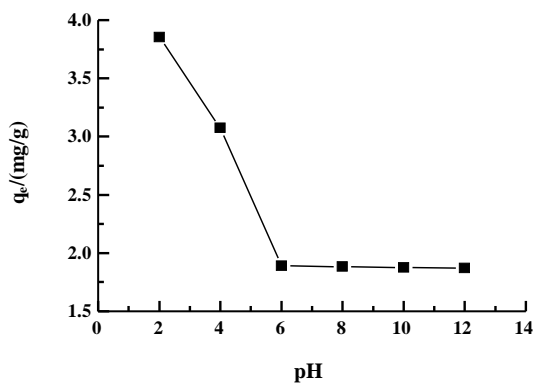
The adsorption experiments were carried out at given contact times for three different initial carmine concentrations at an adsorbent dosage of 2 g/L at temperature  $30 \pm 1\text{ }^{\circ}\text{C}$ . The effect of the rate of adsorption is shown in Fig. 2. The adsorption capacity increased considerably as increasing contact time. The contact time to reach saturation with initial concentration of carmine between 26.5- 65.7 mg/L was approximately 20 h. Fig.2 also shows that the equilibrium capacity of CPH increased from 5.62 to 8.66 mg/g as increasing initial concentration of carmine because the initial carmine concentration provides an important driving force to overcome all mass transfer resistance. The increase of loading capacity of CPH with increasing carmine concentration may also be derived from the higher interaction between carmine and CPH.

### Effect of the adsorbent dosage

Fig. 3 shows the effect of adsorbent dosage on the percent removal efficiency. The percent removal efficiency increased from 43.3% up to 98.5% as the adsorbent dosage increased from 2 to 10 g/L, which can be attributed to increased surface area and the adsorption sites.

Table 1: Thermodynamic properties of the systems tested.

| $q_e$ (mg/g) | $\Delta H$ (kJ/mol) | $\Delta G$ (kJ/mol) |        |        | $\Delta S$ (J/mol·K) |        |        |
|--------------|---------------------|---------------------|--------|--------|----------------------|--------|--------|
|              |                     | 303K                | 313K   | 323K   | 303K                 | 313K   | 323K   |
| 4            | 13.83               | -34.80              | -35.85 | -36.34 | 160.49               | 163.96 | 165.58 |
| 5            | 34.69               |                     |        |        | 229.34               | 232.81 | 234.42 |

Fig. 3: Effect of adsorbent dosage ( $T = 30^\circ\text{C}$ ,  $\text{pH} = 2.0$ ,  $c_0 = 30 \text{ mg/L}$ ,  $\text{rpm} = 150$ ).

Since the particle size range is constant, the surface area will be regularly proportional to the mass of CPH used.

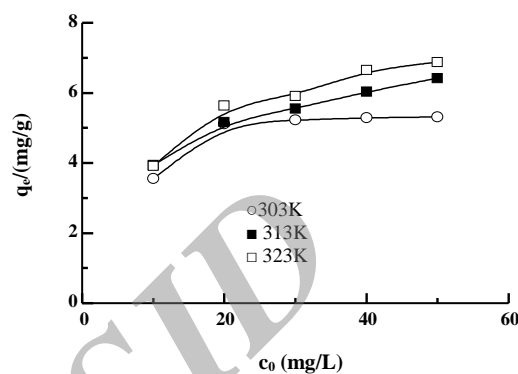
#### Effect of temperature

Removal of carmine by CPH was performed by varying dye concentration from 10-50 mg/L at temperature 303, 313 and 323 K, respectively. Fig. 4 shows that adsorption capacity increased from 3.56 to 5.29 mg/g at 303 K, from 3.9 to 6.03 mg/g at 313 K, and from 3.91 to 6.65 mg/g at 323 K by increasing carmine concentration. At the same temperature, the increased initial carmine concentration resulted in a higher driving force for mass transfer.

Adsorption of carmine on CPH was enhanced by increasing the temperature from 303 K to 323 K at different initial dye concentration. According to Fig. 4, there was an increase in equilibrium adsorption capacity at the same concentration when the temperature was high, due to an endothermic process. Thermodynamic parameters were determined by investigation effect of temperature on carmine adsorption.

#### Thermodynamic parameters

Thermodynamic parameters, i.e. free energy change ( $\Delta G$ ), isosteric enthalpy change ( $\Delta H$ ) and entropy

Fig. 4: Effect of initial dye concentration by CPH (contact time = 24 h,  $\text{pH} = 2.0$ , adsorbent dosage = 2 g/L,  $\text{rpm} = 150$ ).

change ( $\Delta S$ ), vary with the thermodynamic equilibrium constant ( $K$ ) and have been calculated using Eq. (6), Eq. (7) and Eq. (8). The values of thermodynamic parameters are reported in Table 1. The negative values of  $\Delta G$  reveal that the adsorption of carmine is thermodynamically feasible and spontaneous. Positive value of  $\Delta H$  confirms the endothermic nature of the adsorption process. Hence, the adsorption capacity will increase with increasing temperature. The numerical value of  $\Delta H$  also predicts the physisorption behavior which confirms the adsorption theory of Langmuir model. The positive values of  $\Delta S$  reflect the affinity of CPH to carmine and also indicate the increased disorder at the solid/solution interface during the adsorption process.

#### Adsorption Isotherms parameters

The adsorption isotherm studies give information about the capacity of adsorbent to remove dyes. Experimental adsorption equilibrium data in Fig. 4 obtained at 303, 313 and 323 K were fitted with Langmuir model. The plot of  $c_e/q_e$  against  $c_e$  yields straight lines (Fig. 5). The correlative coefficient  $R^2$  values confirm that the adsorption equilibrium data fitted well with the Langmuir model under the studied conditions. This indicates uniform adsorption and strong

Table 2: Isotherms constants for the adsorption of carmine on CPH.

| T (K) | Langmuir constants |              |        | Freundlich constants |      |        |
|-------|--------------------|--------------|--------|----------------------|------|--------|
|       | $q_{\max}$ (mg/g)  | $K_L$ (L/mg) | $R^2$  | $k_F$                | $n$  | $R^2$  |
| 303   | 5.443              | 0.999        | 0.9991 | 3.262                | 6.75 | 0.7968 |
| 313   | 6.090              | 0.960        | 0.9908 | 3.657                | 6.78 | 0.7957 |
| 323   | 6.684              | 0.752        | 0.9874 | 3.615                | 5.60 | 0.8037 |

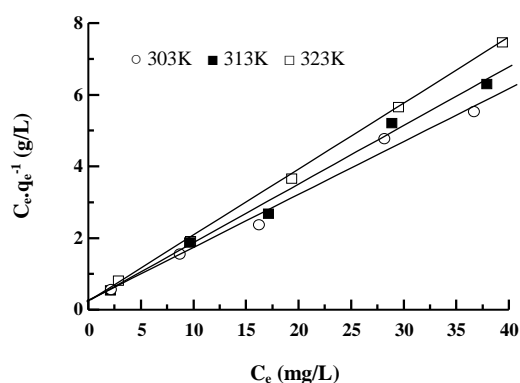


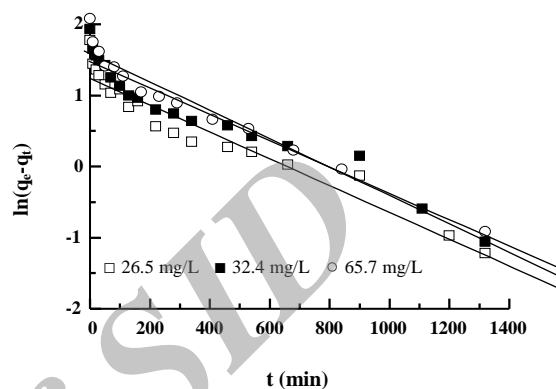
Fig. 5: Fit linear of the Langmuir isotherm.

dye-adsorbent interactions over the surface of the adsorbent. The values of the Langmuir constants  $K_L$ , the monolayer capacity of adsorbent  $q_{\max}$ , and  $R^2$  are listed in Table 2. It was seen that the maximum monolayer capacity of CPH is determined as 5.443, 6.090, 6.684 mg/g for 303, 313 and 323 K, respectively. The  $q_{\max}$  increased with increasing temperature, while equilibrium constant  $K_L$  decreased as temperature increased.

The magnitude of  $R^2$  indicated the inadequacy of Freundlich model to explain the adsorption process. Based on the comparison of  $R^2$ , the adsorption isotherms were better described by the Langmuir equation.

#### Kinetic parameters of adsorption

In order to investigate the adsorption process of carmine onto CPH, pseudo first-order, pseudo second-order and intraparticle diffusion model were used. The plots of linearized form of the pseudo first-order model are in Fig. 6. The values of  $k_1$ ,  $q_{eq}$  and correlative coefficients are compared in Table 3. The correlation coefficients for the pseudo first-order kinetic model were less than 0.95. Moreover, a large difference of equilibrium adsorption capacity ( $q_e$ ) between the experiment and calculation was observed, indicating a poor pseudo first-order fit to the experimental data.

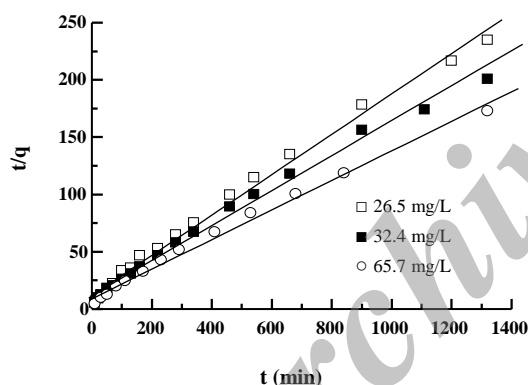
Fig.6: Pseudo-first order adsorption kinetics ( $T = 30\text{ }^\circ\text{C}$ ,  $\text{pH} = 2.0$ , CPH dosage = 2g/L, rpm = 150)

The linearized form of pseudo second-order model is presented in Fig. 7. The rate constant  $k_2$ , the  $q_e$  value and the corresponding linear regression correlation coefficient  $R^2$  under different concentrations were calculated from the linear plots of  $t/q_t$  against  $t$  and the results are given in Table 3. At all initial carmine concentrations, the straight lines with extremely high correlative coefficients ( $>0.99$ ) were obtained. In addition, the calculated  $q_e$  values are also consistent with the experimental data in the case of pseudo-second order kinetics. These reveal that the adsorption data are well represented by pseudo second-order kinetics. From Table 3, the values of  $k_2$  decrease with initial carmine concentration. This may be due to the low competition for the adsorption sites at lower concentration. Similar types of kinetic model parameters were obtained by various researchers in literatures [22-24].

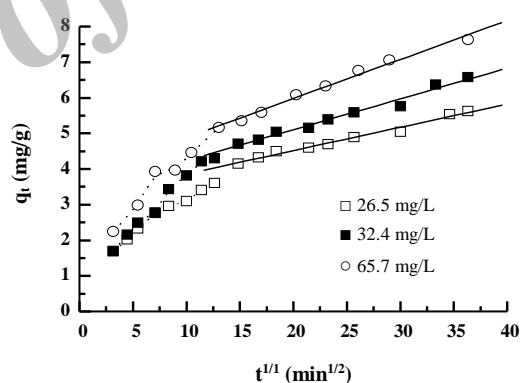
The possibility of intraparticle diffusion cannot be overlooked because of the long adsorption equilibrium time in our experiments. For clear illustration of this, intraparticle diffusion model was proposed to describe the adsorption process (Fig. 8). The time dependence of  $q_t$  in Fig. 8 could be presented in two straight lines which could be well fitted linearly. The multi-linearity

Table 3: Statistical results of the application of the kinetic models.

| Model                                  |             |   | Initial carmine concentration (mg/L) |                        |                        |
|--|-------------|---|--------------------------------------|------------------------|------------------------|
|  |             |   | 26.5                                 | 32.4                   | 65.7                   |
| First order kinetic                    | $k_1$       | Rate constant, $\text{min}^{-1}$                        | 0.0019                               | 0.0019                 | 0.002                  |
|  | $q_{e,cal}$ | Equilibrium capacity mg/g                               | 3.53                                 | 4.29                   | 4.96                   |
|  | $R^2$       | Correlation coefficient                                 | 0.9358                               | 0.9315                 | 0.9498                 |
| Second order kinetic                   | $k_2$       | Rate constant, $\text{g/mg}\cdot\text{min}$             | 0.0023                               | 0.0019                 | 0.0016                 |
|  | $q_{e,cal}$ | Equilibrium capacity, mg/g                              | 5.71                                 | 6.61                   | 7.78                   |
|  | $R^2$       | Correlation coefficient                                 | 0.9934                               | 0.9915                 | 0.9928                 |
| Intraparticle diffusion                | $k_p$       | Rate constant, $\text{mg}/\text{min}\cdot\text{g}$      | 0.0654                               | 0.0865                 | 0.1096                 |
|  | C           | Intercept   | 3.21                                 | 3.37                   | 3.79                   |
|  | $R^2$       | Correlation coefficient                                 | 0.9846                               | 0.9788                 | 0.983                  |
| Wünwald-Wagner intraparticle diffusion | D           | Effective diffusion coefficient, $\text{cm}^2/\text{s}$ | $6.64 \times 10^{-10}$               | $6.08 \times 10^{-10}$ | $4.09 \times 10^{-10}$ |
|  |             | Intercept   | -0.2942                              | -0.3504                | -0.3843                |
|  | $R^2$       | Correlation coefficient                                 | 0.9968                               | 0.9875                 | 0.9625                 |
| $q_{e,exp}$                            |             | Experimental data of the equilibrium capacity, mg/g     | 5.73                                 | 6.70                   | 7.78                   |

Fig. 7: Pseudo-second order adsorption kinetics ( $T = 30\text{ }^\circ\text{C}$ ,  $\text{pH} = 2.0$ ,  $\text{CPH dosage} = 2\text{g/L}$ ,  $\text{rpm} = 150$ ).

supported that the intraparticle diffusion was dominant in carmine adsorption. The  $q_t$  in the first portion showed a rapid increase with time, which is attributed to the rapid external diffusion of dyes to the surface of CPH. The second portion corresponded to the intraparticle diffusion effect. The  $k_p$  values were directly calculated from the slope of the second regression line and the values of  $k_p$ , C and correlation coefficients are also shown in Table 3. It is found that the correlation coefficients for the intraparticle diffusion model are all approximate 0.98. However, the linear plots

Fig. 8: Intraparticle diffusion ( $T = 30\text{ }^\circ\text{C}$ ,  $\text{pH} = 2.0$ ,  $\text{CPH dosage} = 2\text{g/L}$ ,  $\text{rpm} = 150$ ).

at each concentration did not pass through the origin of coordinates, which indicates that the intraparticle diffusion was not the sole rate-controlling step [24-26].

Table 3 showed the calculated results of Wünwald-Wagner intraparticle diffusion model and revealed that the values of the internal diffusion model and revealed that the values of the internal diffusion coefficient fall well within the magnitudes reported in literature [21], which suggested that the adsorption of carmine should be governed by intraparticle diffusion mechanism.

## CONCLUSIONS

In this study, the adsorption of carmine onto peanut husk crosslinked with epichlorohydrin in alkaline medium was investigated from equilibrium, kinetic and thermodynamic aspects. The results indicated that the adsorption capacity of the CPH was considerably affected by temperature, initial carmine concentration and pH value. It is also reported that carmine adsorption increased with temperature up to 323K, and increased with initial carmine concentration up to 65.7 mg/L.

The Langmuir isotherm model provided a better description for the adsorption equilibrium when compared with the Freundlich isotherm equation. The CPH can be used as an effective low-cost agriculture by-product adsorbent for the removal of carmine with its adsorption capacity of 6.68 mg/g at 323 K.

The kinetics of carmine adsorption onto CPH was studied by means of the pseudo-first and pseudo-second order kinetic models. The results showed that the pseudo-second order equation provided a better correlation of the adsorption data. The intraparticle diffusion kinetics gave two linear regions, which indicated that the intraparticle diffusion was not the sole rate-controlling step.

The thermodynamic constants of the process were also evaluated. The positive values of  $\Delta H$  indicated an endothermic process. The negative values of  $\Delta G$  confirmed the spontaneous nature and the positive values of  $\Delta S$  showed the increasing disorder at the solid-solution interface during the adsorption.

## Acknowledgement

The work was supported by the Project Foundation of Chongqing Municipal Education Committee(KJ110724) and the Project Foundation of Chongqing Innovative Research Team Development in University (KJTD201020).

Received : Jan. 20, 2013 ; Accepted : Oct. 21, 2014

## REFERENCES

- [1] Zahrim A.Y., Tizaoui C., Hilal N., [Coagulation with Polymers for Nanofiltration Pre-Treatment of Highly Concentrated Dyes:A Review](#), *Desalination*, **266**: 1-16 (2011).
- [2] Sharma P., Kaur H., [Sugarcane Bagasse for the Removal of Erythrosin B and Methylene Blue from Aqueous Waste](#), *Appl. Water Sci.*, **1**: 135- 145 (2011).
- [3] Han R., Ding D., Xu Y., et al., [Use of Rice Husk for the Adsorption of Congo Red from Aqueous Solution in Column Mode](#), *Bioresour Technol*, **99**: 2938- 2946 (2008).
- [4] Khenifi A., Bouberka Z., Sekrance F., et al., [Adsorption Study of an Industrial Dye by An Organic Clay](#), *Adsorption*, **13**: 149-158 (2007).
- [5] Ansari R., Seyghali B., Mohammad Khah A., Ali Zanjanchi M., [Highly Efficient Adsorption of Anionic Dyes from Aqueous Solutions Using Sawdust Modified by Cationic Surfactant of Cetyltrimethylammonium Bromide](#), *Surfact Deterg.*, **15**:557-565(2012).
- [6] Kumar K.V., Kumaran A., [Removal of Methylene Blue by Mango Seed Kernel Powder](#), *Biochem. Eng. J.*, **27**: 83-93 (2005).
- [7] Robinson T., Chandran B., Nigam P.,[Removal of Dyes from a Synthetic Textile Dye Effluent by Biosorption on Apple Pomace and Wheat Straw](#), *Water Research*, **36**: 2824- 2830 (2002).
- [8] Gong R., Ding Y., Li M., et al., [Utilization of Powdered Peanut Hull as Biosorbent for Removal of Anionic Dyes from Aqueous Solution](#), *Dyes Pigments*, **64**: 187- 192(2005).
- [9] Dursun O., Gulbeyi D., Ahmet O., [Methylene Blue Adsorption from Aqueous Solution by Dehydrated Peanut Hull](#), *Journal of Hazardous Materials.*,**144**: 171-179(2007).
- [10] Romero L.C., Boncomo A., Gonzo E.E., [Acid Activated Carbons form Peanut Shells:synthesis, Characterization and Uptake of Organic Compounds from Aqueous Solutions](#), *Adsorp. Sci. Technol.*, **21**: 617-626 (2001).
- [11] Yinghua Song, Yi Liu, Shengming Chen et al., [Sunset Yellow Adsorption by Peanut Husk in Batch Mode](#), *F. Environ. Bull.*, **23**(4): 1074- 1079 (2014).
- [12] Ricordel S., Taha S., Cisse I. et al., [Heavy Metal Removal by Adsorption Onto Peanut Husks Carbon:Characterization, Kinetic Study and Modeling](#), *Sep. Purif. Technol.*, **24**: 389-401(2004).
- [13] Gonzo E.E., Gonzo L.F., [Kinetics of Phenol Removal from Aqueous Solution by Adsorption onto Peanut Shell Acid Activated Carbon](#), *Adsorp. Sci. Technol.*, **23**: 289- 302 (2005).
- [14] Allen S.J., Gan Q., Matthews R. et al., [Mass Transfer Processes in the Adsorption of Basic Dye by Peanut Hulls](#), *Ind. Eng. Chem. Res.*, **44**: 1942-1949 (2005).



- [15] Gracia-Delgado R.A., Cotoruelo-Minguez L.M., Rodriguez J.J., **Equilibrium Study of Single-Solute Adsorption of Anion Surfactants with Polymeric XAD Resins**, *Sep. Sci. & Technol.*, **27**: 975-987 (1992).
- [16] John P.B., Marios T., **Removal of Hazardous Organic Pollutants by Biomass Adsorption**, *J. Water Pollut. Control Fed.*, **59**: 191- 198 (1987).
- [17] Lagergren S., **About the Theory of So-Called Adsorption of Soluble Substances**, *Kungliga Svenska Vetensk. Handl.*, **24**: 1- 39 (1898).
- [18] Ho Y.S., McKay G., **Pseudo-Second Order Model for Sorption Processes**, *Process Biochem.*, **34**: 451-465 (1999).
- [19] McKay G., **The Adsorption of Dyestuffs from Aqueous Solution Using Activated Carbon: Analytical Solution for Batch Adsorption Based in External Mass Transfer and Pore Diffusion**, *Chemical Engineering Journal*, **27**: 187-196 (1983).
- [20] Weber W.J., Morriss J.C., Sanit J., **Kinetics of Adsorption on Carbon from Solution**, *Eng. Div. Am. Soc. Civ. Eng.*, **89**: 31-60 (1963).
- [21] Kalvathy M.H., Karthikeyan T., Rajgopal S. et al., **Kinetic and Isotherm Studies of Cu(II) Adsorption Onto H<sub>3</sub>PO<sub>4</sub>-Activated Rubber Wood Sawdust**, *Journal of Colloid and Interface Science*, **292**: 354-362 (2005).
- [22] Abd El-Latif M.M., Ibrahim A.M., EI-Kady M.F., **Adsorption Equilibrium, Kinetics and Thermodynamics of Methylene Blue from Aqueous Solutions Using Biopolymer Oak Sawdust Composite**, *J. Am. Sci.*, **6**(6): 267- 283 (2010).
- [23] Vimonses V., Lei S., Jin B. et al., **Kinetic Study and Equilibrium Isotherm Analysis of Congo Red Adsorption by Clay Materials**, *Chemical Engineering Journal*, **148**: 354- 364 (2009).
- [24] Sen T.K., Afroze S., Ang H., **Equilibrium, Kinetics and Mechanism of Removal of Methylene Blue from Aqueous Solution by Adsorption Onto Pine Cone Biomass of Pinus Radiata**, *Water Air Soil Pollut.*, **218**: 499-515 (2011).
- [25] Han X., Niu X., Ma X., **Adsorption Characteristics of Methylene Blue on Polar Leaf in Batch Mode: Equilibrium, Kinetics and Thermodynamics**, *Korean J. Chem. Eng.*, **29**(4), 494-502 (2012).
- [26] Ghaedi M., Tashkhourian J., Pebdani A.A., et al., **Equilibrium, Kinetic and Thermodynamic Study of Removal of Reactive Orange 12 on Platinum Nanoparticle Loaded on Activated Carbon as Novel Adsorbent**, *Ana F.N., Korean J. Chem. Eng.*, **28** (12) 2255- 2261 (2011).